Journal of the Iranian Chemical Society (2022) 19:1–22
https://doi.org/10.1007/s13738-021-02290-0

REVIEW PAPERS

Optical sensors for determination of water in the organic solvents: a review

Abolghasem Jouyban[1,2] · **Elaheh Rahimpour**[1,3]

Received: 4 March 2021 / Accepted: 18 May 2021 / Published online: 24 May 2021

Abstract
In organic solvents, water is the most frequently found impurity. It interferes with many reactions, so it can be a reason for importance of its determination. Karl Fischer titration is a commonly used method for this purpose. However, some disadvantages particularly the inability of continuous analysis limit its applications. The current study reviews the optical sensors/nanosensors developed for the determination of water and demonstrates their applications in checking water impurity in organic solvents. Such optical sensors are highly demanded in the sensing procedures due to their simplicity and low price. Almost these methods do not need any expensive or complicated vehicles. This review focuses on optical sensors/nanosensors for the quantification of water content in organic solvents from 2016 to 2020 and is an update of Jung et al. work in 2016. The reported sensors/nanosensors are categorized into two types: spectrophotometry and spectrofluorimetry; each of them is classified based on the used materials for water sensing. The details of each reported method are explained in this review in detail, and their analytical characteristics are given as a table.

Keywords Sensor · Nanosensor · Water content · Organic solvent

Introduction

Water is the most common impurity in many organic solvents, and its diagnosis is important to most fields such as laboratory chemistry, fine chemical industry, biomedical analysis and food processing. Karl Fisher titration is the popular method for water content quantification in organic solvents [1]. It is originally developed in the 1930s in which water reacts with a reagent and is converted to a non-conductive species. Although this technique has a lot of advantages including absolute measurement, high sensitivity, applicability to both liquid and solid samples, low capital cost, and wide application range [2], some disadvantages including the need for specialized equipment and skilled operator limit its applications [3]. Electrochemical and electrophysical sensors are other sensing mechanisms for the quantification of water content. Their robustness and ease of calibration and use caused to be employed in industrial sectors. However, limitations reported for these methods are a lack of enough precision and portability for real-time analysis and, owing to the electronic nature, are liable to electromagnetic radiation [4]. Compared with above-mentioned techniques, the optical water sensing based on fluorophore or chromophore materials offers an alternative choice owing to numerous advantageous, including simple operability, high sensitivity, easy preparation, and convenient on-site detection.

The current work aims to review various optical sensors and nanosensors for the quantification of water content in organic solvents. The works reviewed here were obtained by searching the SCOPUS database for the years 2016–2020 employing the below search phrases: "fluorometric sensors for determination of water," "colorimetric sensors for determination of water," "nanosensors for determination of water," and "water content in organic solvents." A total of 58 papers related to the subject were chosen for reviewing. This article is an update of Jung et al. work in 2016 [4]. They categorized the methods based on sensing mechanisms including intramolecular charge transfer, photo-induced

✉ Elaheh Rahimpour
rahimpour_e@yahoo.com

[1] Pharmaceutical Analysis Research Center and Faculty of Pharmacy, Tabriz University of Medical Sciences, Tabriz, Iran

[2] Immunology Research Center, Tabriz University of Medical Sciences, Tabriz, Iran

[3] Food and Drug Safety Research Center, Tabriz University of Medical Sciences, Tabriz, Iran

electron transfer, water-induced decomplexation of dyes, proton transfer, solvatochromism, water-induced interpolymer π-stacking aggregation, etc., whereas we classify the reported sensors/nanosensors based on analytical techniques into two types: spectrofluorimetry and spectrophotometry; each of them is categorized based on used materials for water sensing. Herein, we provide some explanations for each method and give their characteristic features as table.

Developed optical sensors/nanosensors for the quantification of water content in the organic solvents

The optical techniques reported for the quantification of water content in organic solvents are classified into two types: spectrofluorimetry and spectrophotometry which are reviewed in detail in the following sections.

Spectrofluorimetric methods

In the sensors/nanosensors based on spectrofluorimetry, a fluorophore senses a variation in its environment and shows a response in either the emission intensity or the wavelength of probe emission. The fluorescence properties of a fluorophore change in the presence of water through a variety of mechanisms including intramolecular charge transfer (ICT), photo-induced electron transfer (PET), excited state intramolecular proton transfer (ESIPT), water as a competitive ligand, aggregation-induced emission, aggregation-based monomer–excimer/exciplex switching, water-induced interpolymer π-stacking aggregation, and hydrogen bond interactions. PET is a dynamic quenching process in which an excited electron is transferred from donor to acceptor in the absence of an analyte (water in this case). PET-based system is generally composed of a receptor attached using a spacer to an energy matched fluorophore. After excitation, charge recombination occurs as a result of the electron transfer process and causes the return to the ground state and thus quenches the fluorescence emission, whereas analyte precludes this procedure [5]. In ICT-based sensors, a receptor attached to an energy matched fluorophore directly and results in fluorescence quenching after excitation of a fluorophore. This procedure precludes in the presence of water due to variation in the dipole strength of the donor–acceptor couple [6]. ESIPT is observed in the planar organic molecules containing acidic and basic functional groups bounded by an intramolecular hydrogen bond (*e.g.,* keto–enol tautomers). In ESIPT procedures and by considering the fact that water possesses both hydrogen bond donor and hydrogen bond acceptor properties, the water adding causes a disruption in the ESIPT systems [7]. Another feature of water is its action as a competitive ligand. Lanthanides show a strong luminescence in the presence of organic ligands due to the antenna effect. However, the excited states of the lanthanide ions are more sensitive to ligation by water and result in quenching the corresponding luminescence and this effect is proportional to the number of water molecules in the lanthanide ion first coordination sphere [8]. Aggregation-induced emission is observed for a compound with a highly conjugated structure with a high degree of rotational freedom which results in quenching the emission using this mechanism [9]. Aggregation with changes in environmental polarity results in the restriction in the structure rotation, thus eliminating the rotational (non-emissive) de-excitation pathway and recovered its fluorescence. Aggregation-based monomer–excimer/exciplex switching is normally observed in flat polycyclic aromatic hydrocarbons and has high affinity for an identical molecule in the ground state for forming an excited dimer structure; their affinity is lowered, after the emission of a photon. Changing in polarity and the viscosity of environmental leads to conformational changes that decrease or increase the intramolecular distance between the monomers and affect the ratios of monomer and excimer fluorescence. As emission profile of excimer differs from that of the monomer, it can be used for analytical purposes [10]. Polymers with a high π-conjugated system are sensitive to their environment and their physical and optical features differ when the environmental polarity is changed, so they can be used as a sensor for polar solvents such as water. Hydrogen bond interaction between a fluorophore and water molecules in an organic solvent can also change the optical properties of fluorophore in that solvent which can be used for water content monitoring. The employed fluorophores in the mentioned water sensing platforms may be (1) dye, (2) lanthanide, (3) upconversion (UC) materials, (4) nanomaterials and (5) other fluorescent compounds; examples of each of them are given in the following sections. The analytical features of the given methods are given in Table 1.

Fluorescent dyes

Kumar et al. [11] used a probe composed of the fluorescent reporter dansyl dye bounded to Fe (III) ion for quantification of water content in tetrahydrofuran (THF), acetone and acetonitrile. Probe of dansyl dye attached with Fe (III) ion is a non-fluorescent species, and it shows a strong emission after adding a trace amount of water. The emission character of ligand was regenerated in the presence of water due to probable displacement of iron from probe with water (Fig. 1). This method shows a linear response to water in the ranges of 0.0–0.049 wt% in THF, 0.0–4.975 wt% in acetone and 0.0–7.729 wt% in acetonitrile. Ooyama et al. [12] reported a boron-dipyrromethene (BODIPY) sensor based on PET mechanism for determination of water content in toluene, 1,4-dioxane, THF, acetone and acetonitrile. They

Table 1 Characteristics of included studies on spectrofluorometric-based methods for determination of water content in organic solvents

Applied material	Measured media	Linear range	LOD	RSD%	Remarks	Ref.
Dansyl dye attached with Fe(III) ion	THF Acetone, Acetonitrile	Up to 0.049 wt% Up to 4.975 Up to 7.729	0.0003 wt% 0.4057 0.1432	NR	The emission character of ligand was regenerated in the presence of water due to probable displacement of iron from probe with water	[11]
(BODIPY) MH-1	Toluene, 1,4-Dioxane THF Acetone Acetonitrile	–	–	NR	The fluorescence enhancement of MH-1 in acetone and acetonitrile with increasing water content in the solution can be attributed to the suppression of the PET process and decrease in fluorescence intensity upon addition of water to the solution for non-polar solvents such as 1,4-dioxane, THF and toluene, the is attributed to the disruption of B–N interaction in MH-1(BN) associated with the formation of ionic species MH-1(H_2O) in the solvent/water mixture	[12]
3,5-Dimethyl BODIPY	1,4-Dioxane, THF Acetone,, Acetonitrile, DMSO	Up to 20% v/v	0.003% v/v	NR	The fluorescence variation of probe in the presence of water is attributed to this fact that the red emissive probe would convert to the aldehyde hydrate (1,1-diol), resulting in significant absorption and emission shifts as the meso-substituent goes from a withdrawing to a donating group and the extent of π-conjugation is reduced	[13]
4-Methylumbelliferone/Sudan I system	Hexadecane	0.03–3.33% v/v	–	NR	The increase of water contents in the sample leads to increase of the emission intensity	[14]
4′-*N*, *N*-dimethylamino-4-methylacryloylamino chalcone optode membrane	Ethanol, Acetone, Tetrahydrofuran	Up to 10% v/v	0.0097% v/v 0.011% 0.017%	NR	Florescence intensity of dye immobilized optode membrane decreased when connecting water due to polarity variation	[15]
Coumarin conjugate	DMSO DMF THF Acetonitrile Acetone Dioxane	Up to 50% v/v	0.095% v/v 0.088% 0.13% 0.024% 0.019% 0.025%	NR	Fluorescence intensity of coumarin conjugate was decreased in the presence of water owing to twisted intramolecular charge transfer	[16]
Cyanostilbene derivative	THF Dioxane	Up to 0.5% v/v Up to 2.0%	0.0063% v/v 0.21%	NR	Florescence intensity of cyanostilbene derivative decreased when connecting water due to polarity variation	[17]

Table 1 (continued)

Applied material	Measured media	Linear range	LOD	RSD%	Remarks	Ref.
Rhodamine B	Ethanol	Up to 10% w/w	< 1.4% w/w	NR	A decrease of the fluorescence intensity and a redshift of the emission bands are observed as a result of the increase in the water content due to the emergence of ethanol–water hydrogen bonds	[18]
Acridinyl dyes	Diethyl ether THF Ethyl acetate DMF Acetone Acetonitrile	–	0.001–0.005% v/v	NR	The fluorescence of probe is decreased in the presence of water due to an increased radiationless relaxation from an intramolecular charge-transfer excited state upon hydrogen bond interaction with water	[19]
Eu (III)-phenanthroline complex	Ethanol	–	32.4 $mg.L^{-1}$	NR	The photoluminescence intensity of complex decreased substantially with the addition of water below 1% (H_2O/ethanol) and the red emission has also been completely quenched (> 90%). The possible mechanism is quenching of lanthanide excited states by high-frequency vibrations of H_2O molecules via non-radiative energy transfer process. Furthermore, the strongly coordinated H_2O molecules might cause a structural change or rearrangement of the europium complex, which would be unsuitable for energy migration from ligand to metal ions	[20]
$Tb_{97.11}Eu_{2.89}$-L1 MOF sensor	Acetonitrile	Up to 2.5% v/v	0.04% v/v	NR	As the water content increases, the fluorescence intensity of Eu^{3+} quenches more significantly than that of Tb^{3+}, which eventually leads to an increase in I_{543}/I_{615}	[21]
Tb^{3+}@p-CDs/MOF nanoprobe	Ethanol DMF Cyclohexane	Up to 30% v/v	0.28% v/v	NR	The ratio of light intensity at 545 nm (related to Tb^{3+}) to that at 605 nm (related to p-CDs) increases linearly with increasing water content	[22]

Table 1 (continued)

Applied material	Measured media	Linear range	LOD	RSD%	Remarks	Ref.
Nitrogen and sulfur codoped carbon-based dots encapsulated into red-light-emitting europium MOF	Ethanol	0.05–4% v/v	0.03% v/v	NR	Water molecules are very efficient quenchers (O – H oscillators) toward the luminescence of Eu^{3+} complexes. As composites emit red light in organic solvents and blue light in water, the ratio of light intensity at 420 nm to that at 623 nm (I_{420}/I_{623}) increases linearly with increasing water content	[23]
R6G@Eu-MOF	DMF Acetonitrile THF Methanol Ethanol Isopropanol, *n*-Butanol	Up to 12.4% v/v Up to 10.0% Up to 1.8% Up to 3.5% v/v – – –	0.085%, v/v 0.094% 0.032% 0.032% 0.028%, 0.016% 0.021%	NR	R6G emission of R6G@Eu-MOF exhibits two different ratiometric sensing mode in protic/aprotic polar solvents due to hydrogen binding between R6G and solvents	[24]
1:Tb	Ethanol, Methanol, Acetonitrile, THF *n*-Heptane	–	1.12% v/v 0.47% 0.04% 0.13% 0.53%	NR	The sensitization has been facilitated by the incorporation of water molecules in the crystal lattice	[25]
Polyethylenimine-modified $NaBiF_4$:Yb^{3+}/Er^{3+} UC NPs	Ethanol	Up to 10.0 v/v	–	NR	Water disintegrated the surface of UC NPs	[26]
BF_4^--modified $LiErF_4$: 0.5% Tm^{3+}@ $LiYF_4$ UCNPs	Acetonitrile DMSO DMF	–	58 ppm 50 ppm 30 ppm	NR	Adsorption of water on the surface of probe nanoparticles, resulting in the significantly quenching of the luminescence	[27]
$NaGdF_4$:Yb,Er@$NaGdF_4$:Yb,Nd nanoparticles with dye sensitized	DMSO, Methanol,, Acetone Acetonitrile, Ethanol	0.05–10% v/v	0.018% v/v	< 1%	The mechanism of this detection is mainly attributed to the amount of NIR dyes adsorbed on the UCNPs surface is affected by water, and the NIR dye transfer efficiency in water is far less than that in the organic phase	[28]
CQDs	Ethanol THF 1,4-Dioxane	0.01–10% v/v	0.01% v/v	NR	Pyridinic-N in the structure of CQDs serves as a stronger acceptor of hydrogen bonds, and increases the possibility of non-radiative relaxation of the excited CQDs and leads to the decrease of fluorescent intensity in the presence of hydrogen bond donating molecules	[29, 30]

Table 1 (continued)

Applied material	Measured media	Linear range	LOD	RSD%	Remarks	Ref.
Nitrogen-doped CDs	Acetonitrile DMF Ethanol	Up to 40% v/v 40–100%	8.92%v/v 12.34% 1.67%	NR	Water molecules can induce fluorescence quenching by the destruction of the electronic state of CDs in organic solvents	[31]
CDs	Ethanol	Up to 1% v/v	0.006% v/v	NR	By the introduction of a small amount of water, the fluorescence of the CDs solution showed a very significant decrease owing to reducing the surface oxidation states	[32]
Cs_4PbBr_6 NCs	*n*-Hexane Dichloromethane Toluene	0.06 to 2.3 μL mL^{-1}	0.031 μL mL^{-1} 0.043 μL mL^{-1} 0.057 μL mL^{-1}	NR	In the presence of trace water, part of Cs_4PbBr_6 NCs (non-fluorescent) was hydrolyzed to $CsPbBr_3$ NCs (strong fluorescent)	[33]
Lignin-derived red-emitting CDs	Ethanol, Acetone, DMSO THF DMF Ether	10–60% v/v	0.36% v/v 0.082% 0.16% 0.338% 0.159% –	NR	Water molecules can induce fluorescence quenching due to the solvent polarity and interactions between various solvents and CDs, particularly hydrogen bonding effects	[34]
Glutathione-stabilized copper nanoclusters	DMF, Acetonitrile, THF	0.0014–0.01% v/v 0.0007–0.01% 0.0005–0.01%	0.00042% v/v 0.0002% 0.00016%	NR	The sensitive fluorescence of copper NCs was quenched in the presence of water due to a reverse process of aggregation-induced enhancement (AIE) mechanism	[35]
A solvent-dependent CDs	Acetone THF Acetonitrile	–	0.19% v/v 0.13% 0.18%	NR	The emission peak of CDs shows continuous red shift with increasing water content	[36]
Silyl-protected copper nanoclusters	Acetonitrile THF DMF Dioxane Ethanol	0.0062–0.19%v/v 0.0066–0.19% 0.0068–0.22% 0.0056–0.21% 0.0059–0.2%	0.0018% v/v 0.0019 0.002 0.0011 0.0018	NR	Luminescence of copper nanoclusters is enhanced in the presence of nanoparticles	[37]
Hydrochromic CDs	Acetone, Acetonitrile, Isopropyl alcohol Butyl alcohol, THF	Up to 5.0% v/v	–	NR	The sensing performance can be attributed to the ability of water to make hydrogen bond interactions with CDs in the presence of either a protic or aprotic solvent environment	[38]
Eu (III)-based luminescent nanosphere	Ethanol	0.05–6.0% v/v	0.002% v/v	± 2.08%	Water molecules act as quenchers and caused a structural rearrangement of the Eu (III) complex, which is not favorable to transfer energy from organic ligands to the metal ion and leads to fluorescence quenching	[39]

Table 1 (continued)

Applied material	Measured media	Linear range	LOD	RSD%	Remarks	Ref.
Ru@MIL-NH_2	Ethanol	Up to 100% v/v	0.02% v/v	NR	Water presence changed LUMO and HOMO of π-conjugate system of Ru@MIL-NH_2 and result in the changed blue emission	[40]
Dansyl-based non-fluorescent Cu complex	Methanol, Acetone, Acetonitrile THF	Up to 0.5% v/v Up to 0.5% Up to 0.3% Up to 0.6%	0.033% v/v 0.052% 0.448% 0.00302%	NR	The fluorescence intensity of probe increased dramatically in the presence of water	[41]
RS-Hg	Acetonitrile	1–5% v/v	–	< 4.39%	Fluorescence of RS-Hg complex can be quenched in the presence of water	[42]
4-Amido-1,8-naphthalimide	Acetonitrile, Ethanol	Up to 30% v/v Up to 40%	1% v/v 2%	NR	Water protonates probe generating cations with strong repulsive fields, thus destabilizing the excimer formation	[43]
$TBTNO_2$ based on TPE	THF Dioxane Ethyl acetate, Diethyl ether	0.1–0.3% v/v 0.05–1% 0.3–0.9% 0.15–0.7%	0.019% v/v 0.076% 0.092% 0.103%	NR	The emission of probe were effectively quenched because of twisted intramolecular charge-transfer mechanism	[44]
BOPIM-1 BOPIM-2	1,4-Dioxane, THF, Acetonitrile Isopropanol, Acetone	0.001–0.1% v/v	–	NR	Introduction of trace amount of water to solvent resulted in fluorescent quenching, accompanied by the red shift of the emission, which was attributed to the formation of TICT excitation of BOPIMs by hydrolysis	[45]
7-Dialkylaminocoumarin oxime	DMF, Acetonitrile	Up to 1 wt%	–	NR	Addition of fluoride to the coumarin oxime solutions leads to the deprotonation of the most acidic = N–O–H hydrogen and almost complete fluorescence quenching based on the dark S1 excited state population in conjugate oximates. Traces of water already result in intense fluorescence recovery of the initial oxime due to back aldoxime base protonation	[46]

Table 1 (continued)

Applied material	Measured media	Linear range	LOD	RSD%	Remarks	Ref.
Zn(hpi2cf)(DMF)(H2O) metal–organic framework	Methanol, Ethanol, Acetone Acetonitrile, THF	–	–	NR	The H-bonding between water and –OH group in hydrated MOF effectively hampers the excited state proton transfer to the imidazole N-atom. So, MOF displays blue emission at 463 nm in the solid state. In contrast, the dehydrated MOF has no interference on intramolecular proton transfer, thus characteristic of keto emission (K*) owing to normal process, showing cyan emission at 493 nm	[47]
AMG probe	Ethanol, Acetonitrile, DMF 1,4-Dioxane	–	–	NR	Since AMG in water is easily protonated, the degree of protonation of AMG and its fluorescence in organic solvents could be controlled by varying the water content	[48]
$Sm(HL_2g)(NO_3)_2$	DMF, Methanol, Acetone	Up to 4% v/v Up to 10% Up to 10%	0.29% v/v 0.65% 0.57%	NR	The mechanism of sensing water by probe Sm2g involved in the degradation of macrocycle H_2L_2g based on the water-induced imine bond (C = N) breakage and decreasing the fluorescence intensity of $Sm(HL_2g)(NO_3)_2$	[49]
TPE-FO TPE-FO-TPE	THF 1,4-Dioxane, DMSO	Up to 10% v/v	11 ppm	NR	The formation of the intermolecular hydrogen bond CQO–H–O can be promoted between the oxygen atom of the fluorenone group and water molecule. The non-radiative deactivation processes of the excited state can be strongly enhanced by the intermolecular hydrogen bonding interactions. As a result, the fluorescence of TPE-FO and TPE-FO-TPE can be efficiently quenched by adding water into organic solvents	[50]
9-MP-BF3	Acetonitrile	Up to 1.2% wt	0.25%wt	NR	Water causes the dissociation of 9-MP-BF3 into 9-methyl pyrido[3,4-b] indole (9-MP) and decrease in its fluorescence	[51]
A coumarin-based Schiff base	DMSO	Up to 1% v/v	0.18% v/v	NR	A coumarin-based Schiff base is hydrolysis in the presence of water and show an increase in its fluorescence intensity	[52]

Table 1 (continued)

Applied material	Measured media	Linear range	LOD	RSD%	Remarks	Ref.
Covalent organic frameworks	Methanol, DMF, Acetonitrile Ethanol	1–50% w/v 7–70% 10–60% 7–50%	0.042% w/v 0.262% 0.653% 0.424%	NR	Fluorescence intensity was decreased in the presence of water due to the hydrogen bonding interaction that occurred between water molecule and the N atom of fluorophores	[53]
P-PBI-P	Dioxane	Up to 4.7% v/v	–	NR	The fluorescence of probe is quenched with increase in water content as a result of environmental change of the fluorescent probe and increased polarity which facilitates the photo-induced intramolecular electron transfer process, and results in decreased fluorescence emission	[54]
Hemiindigo	Dioxane	–	10 ppm	NR	Water forms hydrogen bond with hemiindigo and induces significant fluorescence quenching	[55]
Triazaborolopyridinium derivatives	THF, Acetonitrile, Acetone, DMF			NR	The fluorescence emission of triazaborolopyridinium derivatives is quenched in the presence of water due to both solvent polarity and hydrogen bonding,	[56]
Spironolactone form of aminobenzopyranoxanthenes	THF	0.010–0.125 wt%	–	0.18%	The fluorescence intensity at 520 nm (solvatochromic peak) quantitatively decreased in the presence of water due to polarity changing of probe environmental	[57]
Indium metal – organic polyhedra [In2(TCPB)2]·2H2O	Acetonitrile	–	2.95×10^{-4}% v/v	NR	Luminescence intensity of probe is strongly quenched in the presence of water owing to hydrogen bonding effect	[58]
TPA-DPP-TPA	THF Dioxane	–	31 ppm 171 ppm	NR	The synthesized probe is sensitive to solvent polarity and show a fluorescence quenching in the presence of water molecules	[59]
Uranyl tris nitrato	Acetonitrile	Up to 5% v/v	0.03% v/v	5.0%	The intensity of the peak at 467/487 nm related to uranyl tris nitrato decreased as water content increased in acetonitrile	[60]

Table 1 (continued)

Applied material	Measured media	Linear range	LOD	RSD%	Remarks	Ref.
Spirocyclic form of rhodamine	Acetonitrile THF DMSO DMF	–	0.02% v/v 0.05% 0.09% 0.08%	NR	At a lower concentration of water, the spectral shift can indicate the presence of water due to changes in the solvent polarity of the medium or specific probe–water interactions or both; however, at higher concentrations, the sensing is governed by the spirocyclic ring-opening reaction	[61]
4, 4′-Diamino-4″-methoxytriphenylamine	DMSO, Acetonitrile, Ethanol Methanol	0.244–5%v/v 0.205–5 0.202–5 0.224–4	0.0727 w/w% 0.0636 0.0761 0.0631	0.8–2.1% 0.9–1.9% 1.5–2.7% 1.6–2.7%	The fluorescence intensity of probe continuously decreases with the increase in the water contents due to water creation a new non-radiation relaxation routes to dissipate the excess energy of the probe excited molecules	[62]
N,*N*-Dimethyl benzylamine–palladium(II) curcuminate complex	DMSO Ethanol Methanol Acetonitrile	0.08–13.8% v/v 0.03–14.5 0.1–25.0 0.07–18.8	0.01% v/v 0.001 0.05 0.004	1.7% 2.2 2.4 2.5	The fluorescence of complex is quenched in the presence of water due to physical interactions such as hydrogen bonding between water molecules and the excited state of complex	[63]

NR not reported

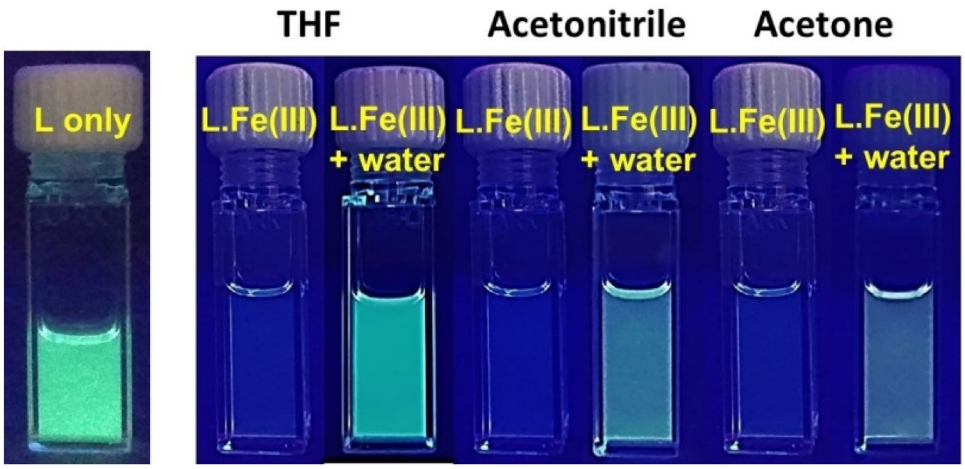

Fig. 1 Fluorescence off–on response and naked eye recognition of L.Fe(III) in dry and wet solvents such as THF, acetonitrile and acetone viewed under the UV lamp. Reproduced with permission from the publisher

show that BODIPY-MH-1 with a PhenylBPin unit can be a fluorescent sensor for low concentration of water with both fluorescence enhancement and attenuation systems. The fluorescence enhancement of MH-1 in acetone and acetonitrile with increasing water content in the solution can be related to the inhibition of the PET process by formation of MH-1(H_2O), which is owing to the lowering of the HOMO level of tertiary amino group by the water adding. On the other hand, for nonpolar solvents including THF, 1,4-dioxane, and toluene, the emission decreasing by water adding to the solution is related to the disruption of B–N interaction in MH-1(BN) along with the formation of ionic species MH-1(H_2O) in the water/solvent mixture. Another similar work was performed by Tae-Il Kim and Youngmi Kim [13] and using 3,5-dimethyl BODIPYs for determination of water with LOD of 0.003% v/v in 1,4-dioxane, THF, acetone, acetonitrile and dimethyl sulfoxide (DMSO). Kłucińska et al. [14] reported a 4-methylumbelliferone/Sudan I system for quantification of water content in the model solvent of hexadecane. The fluorescence spectrum of the donor molecule (4-methylumbelliferone) depends effectively on the water content—its position is affected by protolytic reactions occurring between water and fluorescent dye in lipophilic solvent media. So, the overlapping the emission band of the donor with absorption peak of the acceptor scales with the water amount and the increase of water contents in the sample leads to an increase in the emission intensity. For the maximum wavelength at 540 nm, a linear relationship of fluorescence intensity to water concentration was observed from 0.03 to 3.33% v/v. Other similar studies including using 4′-*N*, *N*-dimethylamino-4-methylacryloylamino chalcone for the quantification of water content in ethanol, acetone, and THF [15], using coumarin conjugate for determination of water content in DMSO, dimethylformamide (DMF), THF, acetonitrile, acetone and dioxane [16], using cyanostilbene derivative for quantification of water content in THF and dioxane [17] using rhodamine B for determination of water content in ethanol [18] and using acridinyl dyes for quantification of water in diethyl ether, THF, ethyl acetate, DMF, acetone and acetonitrile [19].

Lanthanides

Lu et al. [20] reported that Eu (III) in the complexation with phenanthroline shows a high sensitivity to solvent polarity and the detection of trace amount of water through an "on–off" change. It is shown that the photoluminescence intensity of complex decreased substantially with the addition of water below 1% (H_2O/ethanol) and the red emission has also been completely quenched (> 90%). The possible mechanism is quenching of lanthanide excited states by high-frequency vibrations of H_2O molecules via nonradiative energy transfer process. Additionally, the strongly coordinated H_2O molecules might cause a structural change or rearrangement of the europium complex, which would be unsuitable for energy migration from ligand to metal ions. The LOD for this method was reported to be 32.4 mg.L^{-1}. Li et al. [21] reported a $Tb_{97.11}Eu_{2.89}$-L1 metal-organic framework (MOF) sensor that enables ratiometric quantification of water amount in acetonitrile. $Tb_{97.11}Eu_{2.89}$-L1 shows variable colors at different water amounts (0% to 17.6%) with the naked eye. By excitation at 280 nm, $Tb_{97.11}Eu_{2.89}$-L1 displays distinctive transitions of Tb^{3+} and Eu^{3+} ions in dry acetonitrile. Similar to the fluorescence behaviors of Tb-L1 and Eu-L1, the fluorescence intensity of sensor enhanced upon contacting water in acetonitrile. Increasing water amount in acetonitrile causes a decrease in the fluorescence intensities of Tb^{3+} and Eu^{3+} and a rising in that of the ligand. With increase in water amount in the range of 0% to 2.5% (v/v%), the characteristic fluorescence displays an intensity reduction of 75% for the $^5D_0 \rightarrow {}^7F_2$ transition of Eu^{3+}, 18% for the $^5D_4 \rightarrow {}^7F_5$ transition of Tb^{3+} and an increase of 345% for the ligand. Consequently, $Tb_{97.11}Eu_{2.89}$-L1 MOF sensor provides a good linear regression between the emission ratios

(I_{543}/I_{615}) and the water amount in the range of 0%–2.5%, demonstrating that $Tb_{97.11}Eu_{2.89}$-L1 MOF sensor is a helpful tool for the quantification of water amount in an organic solvent. With increasing water content, the emission intensity of Eu^{3+} quenches more effectively than that of Tb^{3+}, which consequently causes a rising in I_{543}/I_{615}. Wu et al. [22] synthesized the p-carbon dots (p-CDs) with strong red-light fluorescence and encapsulated it into a MOF, followed by post-synthetic introduction with green-light-emitting Tb ions to produce two-color light-emitting hybrid (Tb^{3+}@p-CDs/MOF). They reported that the synthesized dots are aggregated easily in water, which leads to a very low fluorescence. When Tb^{3+}@p-CDs/MOF composites are irradiated with energy at an excitation wavelength of 360 nm, the material dispensed in the organic solutions (such as ethanol, DMF and cyclohexane) produces both red and green light, but the luminous intensity of the p-CDs is stronger and eventually shows a red fluorescent color, while dispensed in the aqueous media, owing to agglomeration impact, making red light quenching, finally leaving only green light and thus showing the green light color (Fig. 2). The ratio of emission intensity at 545 nm (related to Tb^{3+}) to that at 605 nm (related to p-CDs) increases linearly with increasing water amount in the range of 0.0% to 30.0% with LOD of 0.28%. Another similar work was done by Dong et al. [23] using nitrogen and sulfur codoped carbon-based dots encapsulated into red-light-emitting europium MOF for determination of water amount in ethanol in the range of 0.05 to 4% v/v with LOD of 0.03%.

Li et al. [24] prepared a dual-emitting fluorescent detector by incorporating a fluorescent dye Rhodamine 6G (R6G) with strong green light emission within a red-light-emitting Eu-MOF through "bottle around ship" technique. Fluorescence spectra of R6G@Eu-MOF in DMF (as an aprotic polar media) and methanol (as a protic polar media) were investigated. The emission intensity of R6G in R6G@Eu-MOF hardly changed within 70 s in DMF. After water adding, the fluorescence intensity of R6G in R6G@Eu-MOF enhanced rapidly, showing that water could improve the release of R6G from Eu-MOF in DMF, whereas the emission intensity of R6G increased to the maximum within 70 s in methanol, and it remained almost unchanged after water adding, which shows that part of R6G could be fast released from Eu-MOF in methanol. This fact is due to presence of an intramolecular hydrogen bonding impact between R6G and the protic polar solvent, which leads R6G partially released into the solvent. However, there is no hydrogen bonding between the aprotic polar solvent DMF and R6G. After water adding, due to the hydrogen bonding between R6G and water, R6G was released slowly and the fluorescence gradually increases. These results showed that the R6G fluorescence of R6G@Eu-MOF displays two different ratiometric sensing modes in aprotic / protic polar media (Fig. 3). Majee et al. [25] synthesized a MOF ($[Y_{1.0}Mn_{1.5}(PDA)_3(H_2O)_3]\cdot_{3.5}H_2O$), named 1, (PDA = 2,6-pyridinedicarboxylic acid) through hydrothermal process and doped it with 10 % terbium ($([Y_{0.9}Tb_{0.1}Mn_{1.5}(PDA)_3(H_2O)_3]\cdot_{3.5}H_2O$), 1:Tb. They reported that the weak metal center fluorescence intensity of dehydrated 1:Tb in organic solvents ethanol, methanol, acetonitrile, THF and n-heptane displayed a large turn-on by increasing water amounts in these solvents. The fluorescence intensity of Tb^{3+} center was improved by several times with a LOD of 1.12 %(v/v), 0.47 %(v/v), 0.04 %(v/v), 0.13 %(v/v) and 0.53 %(v/v), respectively. The studies show that

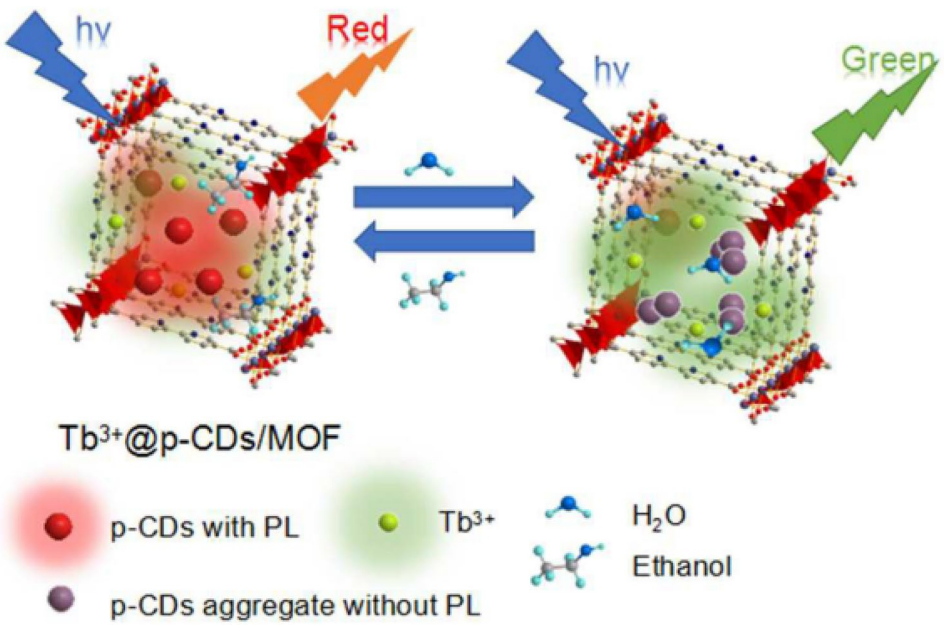

Fig. 2 Mechanism of the photoluminescence response of Tb^{3+}@p-CDs/MOF toward water in organic solvents. Reproduced with permission from the publisher

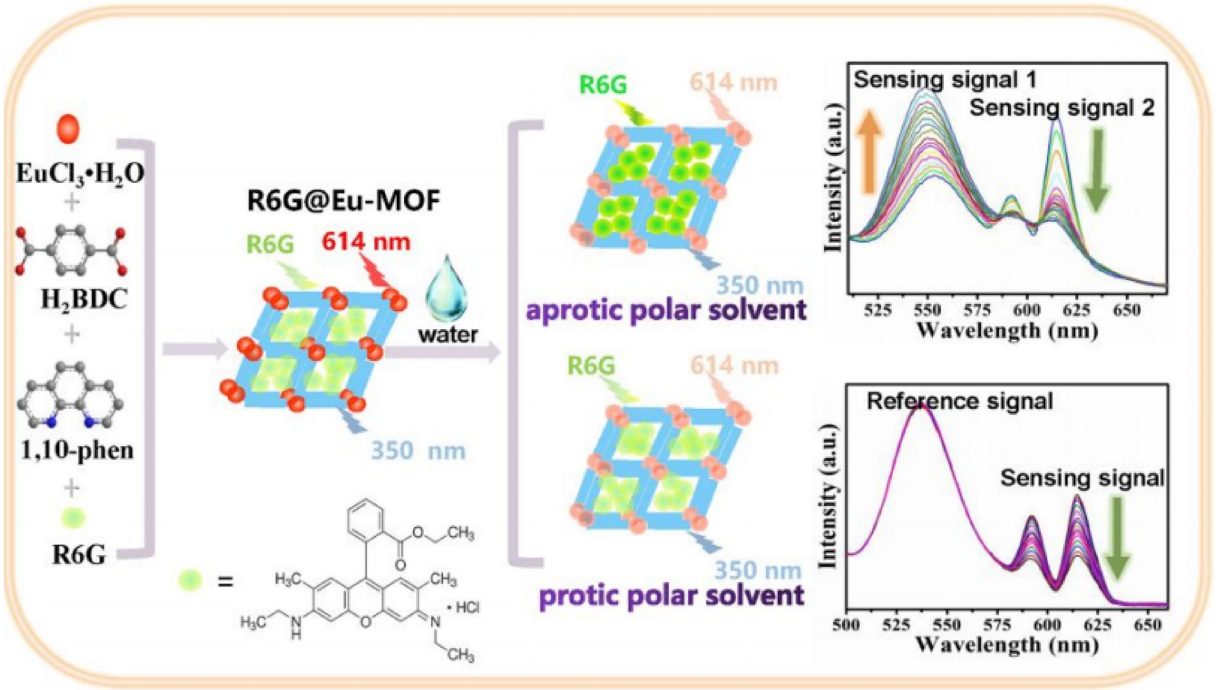

Fig. 3 Illustration of the fabrication of R6G@Eu-MOF and fluorescence detection of water content in organic medium. Reproduced with permission from the publisher

the light is absorbed by the ligand PDA and then by some non-radiative procedure, the energy is transferred to the Tb^{3+} center, and eventually, it observes the green emission from the Tb^{3+} center. So, it can be said that the enhancement has been facilitated by the entering water molecules in the lattice of crystal and the coordination position of Mn. The Mn metal present in 1:Tb is coordinated to two water molecules, and other water molecules have produced a H-bonding network among the PDA ligands and themselves. These existing coordinated and lattice molecules of water cause the structure to be rigid which is a prerequisite for a well enhancement procedure.

Upconversion materials

Pan et al. [26] synthesized polyethylenimine-modified $NaBiF_4$:Yb^{3+}/Er^{3+} UC nanoparticles (NPs) with a hollow structure and used it as a fluorescent probe to determine water amount in organic solvents. They reported that in pure ethanol, fluorescence intensity of UC NPs is the strongest and decreases with water content increase in used ethanol; so that in pure water, fluorescence intensity is the lowest and even is not detectable. Transmission electron microscopy (TEM) results showed that UC NPs were piled closely and maintain hexagonal in neat ethanol (Fig. 4a, d). However, when NPs were placed into a water–ethanol solution, the surface of the NPs was clearly decomposed into a zigzag and the piled nanoplates became separated (Fig. 4b, e). After placing in water or water–ethanol solution with a volume ratio of 1:1 for 12 h, UC NPs disintegrated hardly and hollow structures of them became more obvious and the nanoplates transformed into smaller NPs. This method can be monitored water amount in ethanol solution from 0.0 to 10.0 % v/v. Zhang et al. [27] synthesized BF_4^--modified $LiErF_4$: 0.5% Tm^{3+}@$LiYF_4$ UC nanoprobe for quantification of water amount in acetonitrile, DMSO and DMF. UC NPs exhibit a positive charge that is ascribed to the uncoordinated rare earth metal Er^{3+} cations related to the removal of organic ligands. The electron density of oxygen atom (O) in DMSO or DMF molecules is higher than that of nitrogen atom (N) in acetonitrile, so the interaction between the DMF or DMSO and the BF_4^--coated NPs is stronger than that in acetonitrile. When the water amount is low, owing to the shielding effect of the inner DMF or DMSO molecules, the water molecules place far away the Er^{3+} emission centers, so it is hard to decrease the emission, while in acetonitrile solutions, due to the weak interaction between acetonitrile molecules and BF_4^--coated NPs, water molecules are more easily diffused and adsorbed on the probe NPs surface and cause to quench the fluorescence at very low water amount. The LOD in DMF, DMSO and acetonitrile was 58, 50 and 30 ppm, respectively,

Wang et al. [28] developed a UC material composed of $NaGdF_4$:Yb,Er@$NaGdF_4$:Yb,Nd nanoparticles with dye

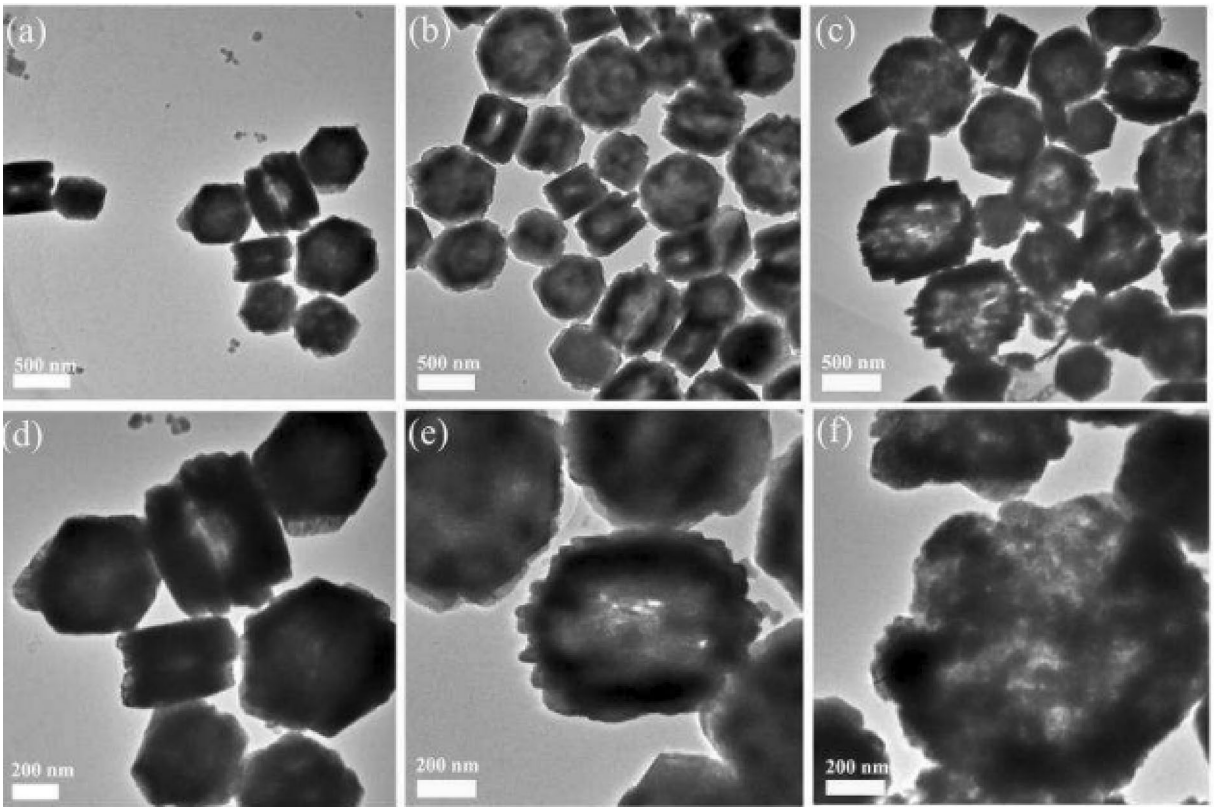

Fig. 4 TEM images of PEI-UC NPs in pure ethanol (**a**, **d**), a mixture of water and ethanol (V:V = 1:1) (**b**, **e**) and a mixture of water and ethanol (V:V = 1:1) (**c**, **f**) after 12 h, respectively. Reproduced with permission from the publisher

enhanced nanoprobe for determination of water amount in DMSO, methanol, acetone, acetonitrile and ethanol. They reported that by water adding to dye-UC NPs in organic solvents, the fluorescence lifetime of the dye-UC NPs–water became shorter than that of the dye-UC NPs, demonstrating that the energy transfer efficiency from the dye to the UC NPs was decreased. However, by adding different water amounts into the dye-UC NPs dispensed in organic solvents, the dye absorption in the supernatant increased, showing that the surface of the IR-808 dye connected to the UC NPs was affected by water. According to the mentioned results, the detection mechanism is mainly ascribed to the amount of NIR dyes adsorbed on the UC NPs surface that is affected by water, and the NIR dye transfer efficiency in water is far less than that in the organic phase. This method shows a linear response to water from 0.05% to 10% v/v with LOD of 0.018% v/v.

Nanomaterials

Wei et al. [29, 30] synthesized carbon quantum dots (CQDs) with yellow emission for determination of water amount in ethanol, THF and 1,4-dioxane. They show that fluorescence of CQDs is quenched by water adding. The reported mechanism for this quenching is as follows: there is pyridinic-N in the structure of CQDs and as the electron density around pyridinic-N is higher, this atom acts as a stronger acceptor of hydrogen bonds, which raises the possibility of non-radiative relaxation of the excited CQDs and causes the quenching of the fluorescent emission in the presence of hydrogen bond donating molecules, such as water. In a word, the emission intensity reduction is ascribed to the specific water–fluorophore interaction and partially to the raising solvent polarity resulting in the water adding. This method can be used for determination of water in the concentration from 0.01 to 10% v/v with LOD of 0.01% v/v. Lee et al. [31] synthesized nitrogen-doped CDs using para-phenylenediamine and nitrilotriacetic acid by solvothermal method. They reported that the emission properties of CDs are controlled easily by the polarity of solvents. Water molecules can induce fluorescence quenching by the disruption of the electronic state of CDs in the organic solvents in three ways. First, by water adding to the organic solvents, the CDs are aggregated due to the low dispersion of CDs in water, which cause quenching resulting in the excessive resonance-energy transfer and π−π interaction. Second, the strong interaction between high polar solvents with para-phenylenediamine in CDs may enhance the rates

of non-radiative decay. Finally, water-induced swelling leads fluorescence quenching, because swelling and shrinking are typical procedures in graphene-like nanomaterials due to the conformational change of CD molecules. Furthermore, water molecules that are as hydronium ions in multilayers of CDs, have the role of an electron-withdrawing compound, which can cause fluorescence quenching. Two linear ranges from 0 to 40% and 40 to 100% water amount are observed for used probe for determination of water in acetonitrile, DMF and ethanol.

Ye et al. [32] synthesized carbon nanodots (CDs) by one-step solvothermal technique and used them for quantification of water amount in ethanol. They found that by adding small water amount, the luminescence of the CDs solution presents a very significant reduction owing to reducing the surface oxidation states. The method offers a good linear response in the water concentration range of 0–1% with LOD of 0.006%. Li et al. [33] reported a smartphone-based ratiometric luminescence device for quantification of trace water in hydrophobic organic solvents such as n-hexane, dichloromethane and toluene. By water adding, part of Cs_4PbBr_6 nanoclusters (NCs) (non-fluorescent) was converted to $CsPbBr_3$ NCs (strong fluorescent). The hydrolysis degree of Cs_4PbBr_6 NCs in a short time (< 1 h) is increased proportional to increasing water amount. This method shows a good response for water with LOD of 0.031, 0.043, and 0.057 μL mL^{-1} in n-hexane, dichloromethane and toluene, respectively.

Other studies include using lignin-derived red-emitting CDs for quantification of water amount in ethanol, acetone, DMSO, THF, DMF and ether [34], using glutathione-stabilized copper nanoclusters for quantification of water amount in DMF, acetonitrile and THF [35], using a solvent-dependent CDs for quantification of water amount in acetone, THF and acetonitrile [36], using silyl-protected copper NCs quantification of water amount in acetonitrile, THF, DMF, dioxane and ethanol [37], using hydrochromic CDs quantification of water amount in acetone, acetonitrile, isopropyl alcohol, butyl alcohol and THF [38] and using luminescent nanospheres of europium (III) mixed complex with 2-thenoyltrifluoroacetone and 1,10-phenanthroline for determination of water amount in ethanol [39].

Other fluorescent compounds

Yin et al. [40] prepared a guest-encapsulation MOF with 2-aminoterephthalic acid, $AlCl_3$ and $Ru(bpy)_3^{2+}$ (Ru@MIL-NH_2) by a simple one-pot technique and used it as a probe for quantification of water amount in ethanol. Ru@MIL-NH_2 shows dual emission at 465 and 615 nm under single excitation of 300 nm. Ru@MIL-NH_2 have a lot of hydrophilic active sites like as aluminum cluster and free –NH_2, so water molecules enter cages easily. Water displaced ethanol molecule and produced the hydrated form of Ru@MIL-NH_2 with water adding. The LUMO and HOMO of π-conjugate system of Ru@MIL-NH_2 changed to produce the changed blue fluorescence. The emission at 465 nm was increased gradually, whereas the emission around 615 nm kept stable relatively under single excitation of 300 nm with water adding from 0 to 100% v/v. Kumar et al. [41] synthesized a dansyl-based non-fluorescent metal complex 1.Cu (Fig. 5) and used it for the quantification of a water amount in organic solvents. 1.Cu is a non-fluorescent compound that its fluorescence intensity increased dramatically in the presence of water in the range of 0.1 to 3.6 % in methanol, acetone, acetonitrile and THF (Fig. 5).

Hu et al. [42] synthesized rhodamine B-based sensor (RS) by a combination of the spironolactone rhodamine B (fluorophore) and multidentate chelates (thiophene and triazole).

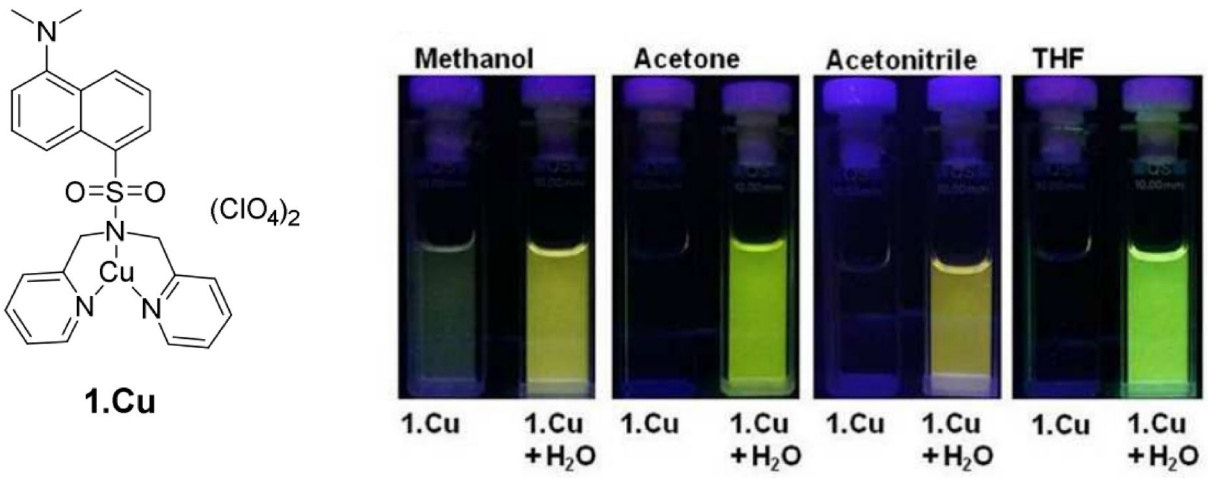

Fig. 5 Structures of receptor 1.Cu, fluorescence off–on behavior of probe 1.Cu as a function of water in methanol, acetone, acetonitrile and THF at $\lambda_{ex} = 345$ nm. Reproduced with permission from the publisher

They show that Hg^{2+} ions can easily form a complex with this compound and have a "turn-on" effect on it. The proposed mechanism is the chelation of Hg^{2+} with RS which induces the spirolactam opening and causing the emission of fluorescence. However, fluorescence of RS-Hg complex can be quenched by adding various concentrations of water (1–5% v/v).

Georgiev et al. [43] proposed a fluorescent probe based on 4-amido-1,8-naphthalimide for quantification of water in ethanol and acetonitrile solvents. The diagnosing mechanism is based on excimer-monomer switching mechanism. Water adding leads to a reduction in the excimer emission centered at about 560 nm and an increase of the monomer emission at 460 nm (Fig. 6). This curious fact could be easily rationalized based on this suggestion that the water protonates probe generating cations with strong repulsive fields, thus destabilizing the excimer formation. The linear range of the observed with this probe for water was 0–30% in acetonitrile and 0–40% in ethanol. Sun et al. [44] synthesized thiazole derivative 2-(4-nitrophenyl)-6-(1,2,2-triphenylvinyl) benzo[d] thiazole ($TBTNO_2$) based on tetraphenylethene (TPE) and used it as a probe for quantification of water amount in THF, dioxane, ethyl acetate and diethyl ether. $TBTNO_2$ shows a strong fluorescence peak in the investigated solvents, and its emissions were effectively quenched when the water amount reached 2% (v/v) due to twisted ICT mechanism linearly with the increase in the water amount in the range of 0.1%–0.3% for THF, 0.05% to 1% for dioxane, 0.3% to 0.9% for ethyl acetate and 0.15% to 0.7% for diethyl ether, respectively.

Other studies for application of fluorescent compounds in the presence of water included using two new boron-fluorine derivatives bearing dimethylamino moieties, BOPIM-1 and BOPIM-2 for determination of water in five organic solvents, THF, 1,4-dioxane, isopropanol, acetonitrile, and acetone [45], using 7-dialkylaminocoumarin oxime for quantification of water in DMF and acetonitrile [46], using Zn(hpi2cf)(DMF)(H_2O) MOF for quantification of water in methanol, ethanol, acetone, acetonitrile and THF [47], using anthracene-based fluorescent water-content chemosensor containing a guanidine moiety (AMG) for quantification of water in ethanol, acetonitrile, DMF and 1,4-dioxane [48], using fluorescent Schiff-base macrocyclic mononuclear Sm(III) complex Sm-2g [$Sm(HL_2g)(NO_3)_2$] for quantification of water in DMF, methanol and acetone [49], using fluorenone-tetraphenylethene luminogens, 2-(4-(1,2,2-triphenylvinyl) phenyl)-9Hfluoren-9-one (TPE-FO) and 2,7-bis(4-(1,2,2-triphenylvinyl)phenyl)-9H-fluoren-9-one (TPE-FO-TPE) for determination of water in THF, 1,4-dioxane, and DMSO [50], using 9-methyl pyrido[3,4-b]indole-boron trifluoride complex (9-MP-BF3) for quantification of water content in acetonitrile [51], using a coumarin based Schiff base for determination of water content in DMSO [52], using a highly crystalline covalent organic frameworks produced by condensation of 1, 3, 5-tris (4-aminophenyl) benzene with 4, 40-biphenyldicarboxaldehyde for quantification of water content in methanol, DMF, acetonitrile and ethanol [53], using pentiptycene (P) and perylene bisimide (PBI)-contained fluorescent dyad (P-PBI-P) for determination of water content in dioxane [54], using hemiindigo for quantification of water content in dioxane [55], using triazaborolopyridinium derivatives for quantification of water amount in THF, acetonitrile, acetone and DMF [56], using spironolactone form of aminobenzopyranoxanthenes for quantification of water amount in THF [57], using indium metal−organic polyhedra [In_2(1,3,5-tri(4-carboxyphenoxy) benzene (TCPB))$_2$]·$2H_2O$ for quantification of water amount in acetonitrile [58], using a donor–acceptor–donor-type diketopyrropyrrole derivative (TPA-DPP-TPA) for quantification of water amount in THF and dioxane [59], using uranyl tris nitrato, i.e., $[UO_2(NO_3)_3]^-$, for quantification of water amount in acetonitrile [60], using spirocyclic form of rhodamine for quantification of water amount in acetonitrile, THF, DMSO and DMF [61] using 4, 4′-diamino-4″-methoxytriphenylamine for determination of water in DMSO, acetonitrile, ethanol and methanol [62] and using

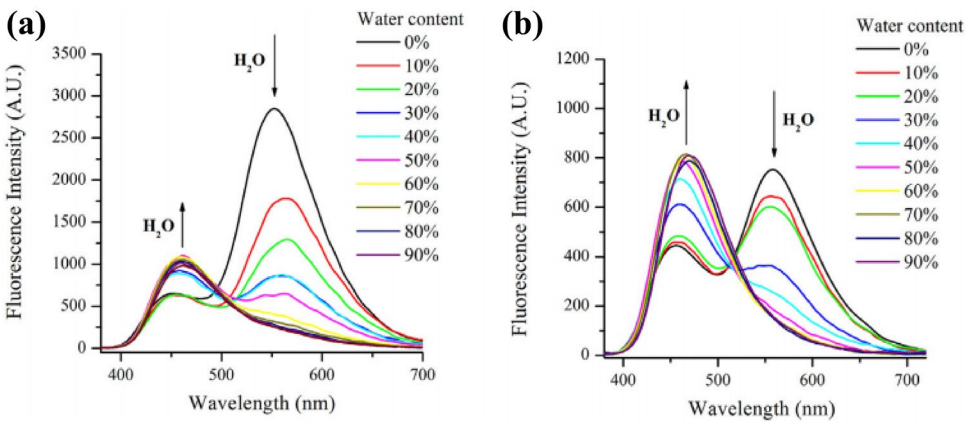

Fig. 6 Influence of the water content on the fluorescent spectra (λ_{ex} = 360 nm) of probe in acetonitrile (**a**) and ethanol (**b**). Reproduced with permission from the publisher

fluorescent *N*,*N*-dimethyl benzylamine–palladium(II) curcuminate complex for water determination in DMSO, ethanol, methanol and acetonitrile [63].

Spectrophotometric methods

In the sensors/nanosensors based on spectrophotometry, the optical properties of a chromophore dissolved in organic phase change in the presence of water as an analyte. Water detection mechanism in these systems can be due to hyperchromism of absorbance band of chromophore with changing in solvent polarity after water adding, protonation of deprotonated form of chromophore, and dissociation of metal-ligand (chromophore) complex in the presence of water. Each of these processes leads to color changing in the utilized system which is detectable with spectrophotometry. The absorbance-based platforms for water sensing can be in both UV-Vis or near infrared (NIR) regions; examples of each of them are given below and the analytical characteristics of the reported methods are summarized in Table 2.

UV–Vis spectrophotometric methods

Tiwari et al. [64] synthesized a simple Schiff base (E)-1-(2,4-dinitrophenyl)-2-(1-(2-hydroxyphenyl)ethylidene) hydrazine-1-ide (DPH) and used it for a colorimetric platform for the signaling of water amount in some water-miscible aprotic organic solvents (acetonitrile and THF). They reported that DPH shows a red color in acetonitrile and THF solutions, whereas its solution in 8% aqueous acetonitrile exhibits dark yellow color and shows a band at 384 nm. The hyperchromism of the band at 363 nm by water adding is related to the protonation of DPH and hence $\pi \rightarrow \pi^*$ electronic transitions of HDPH become prominent at 384 nm. Therefore, the conversion of deprotonated form (DPH) to protonated form (HDPH) by water adding can be used in the quantification of water amount in the range of 0–6% in aprotic organic solvents (Fig. 7).

Kumar et al. [65] reported colorimetric probes based on Alizarin Red S and Sudan-III for the determination of water content in organic solvents such as acetone, THF, DMSO and acetonitrile. These solutions are deprotonated by using fluoride anion and show dramatic color changes. However, the deprotonated forms of solutions are re-protonated by using a trace amount of water (Fig. 8). The LOD of water for Sudan- III was found to be 0.0042 %, 0.0119 %, 0.0058 % and 0.0299 %, and for Alizarin Red S, the detection limits are 0.0221%, 0.0498 %, 0.0850% and 0.5592 % in acetone, acetonitrile, THF, and DMSO, respectively. This research group also used the 1,4-dihydroxy-9,10-anthraquinone or quinizarin-fluoride system with the same mechanism for quantification of water amount in acetonitrile and THF solutions [66].

Another similar work was reported by Wu et al. [67] using hydroxyl-containing polyimides for determination of water contents in DMSO and DMF. The used system is polyimides and fluoride ion complex. Fluoride adding to the polyimides solution leads to the deprotonation of hydroxyl groups of polyimides and color changing to yellow. The deprotonation progress between F^- and OH is easily abrupt by little amount of water owing to high hydration energy of F^- in water. So, the addition of little amount of water into the DMF/DMSO solutions of polyimides causes the UV–Vis absorption spectra to nearly recover to the original state of pure polyimides solutions and visual color changes. Other studies with similar detection mechanism include using coumarin phenylsemicarbazones for determination of water amount in the concentration range of 0–0.36 v/v% in acetonitrile [68], using adenine-linked naphthalimide for quantification of water amount in acetonitrile, THF, DMSO and acetone with LODs of 0.1086%, 0.1936%, 0.4012% and 0.3058% v/v, respectively [69], using diketopyrrolopyrrole-based luminogen for determination of water content by ESIPT mechanism in THF, acetone and acetonitrile with LODs of 0.0064 %, 0.042 %, and 0.192 %, respectively [70], and using indenopyrazine (1)/indenoquinoxaline (2) appended acylhydrazones for determination of water amount in DMF in the range of 0–7.40% and 0–5.21% v/v, respectively [71].

Tan et al. [72] synthesized a molecular sensor with chalcone segment that can attach to metal nitrates selectively (metal = Zn^{2+}, Ni^{2+}, Co^{2+}, Cd^{2+}) with a significant color change from yellow to purple and the selected two-component probe, probe/Ni $(NO_3)_2$, can determine water amount in acetonitrile, acetone, isopropanol and ethanol solvents with re-changing color to yellow (Fig. 9) due to complex dissociation in water. This method shows a linear relationship with water content within the range of 0–10% with the LODs of 0.20%, 0.38%, 0.24% and 0.09% v/v in acetone, acetonitrile, ethanol and isopropanol, respectively. Kumar and Jose [73] synthesized a dabsyl-thiophene-based receptor (E)-4-((4-(dimethylamino) phenyl)diazenyl)-*N*,*N*-bis(thiophen-2-ylmethyl)benzenesulfonamide (DABT) and used for quantification of water amount in THF, acetone, and acetonitrile. Based on ICT in the excited state, the receptor dabsyl-thiophene (yellow color) attached to the mercury ions (magenta color) to stimulate a colorimetric response. The mercury complex is utilized as a moisture probe owing to the dissociation of mercury from probe DABT-Hg by water adding. The sensor shows higher sensitivity to water in THF (LOD = 0.0041% w/w), acetonitrile (LOD = 0.1008% w/w) and acetone (LOD = 0.0144% w/w). Yoo and Kim [74] synthesized a stable water sensor by encapsulation of a functional organic azo dye ((E)-4-((4-(dimethylamino) phenyl)diazenyl)-1-propylpyridin-1-ium bromide) in a rigid host ($AlPO_4$-5 nanochannel). $AlPO_4$-5 not only has a host role but also facilitated the dissociation of water molecules

Table 2 Characteristics of included studies on spectrophotometric based methods for determination of water content in organic solvents

Applied material	Measured media	Linear range	LOD	RSD %	Remarks	Ref
DPH	Acetonitrile THF	Up to 6% v/v	0.28% v/v	NR	Deprotonated form of DPH is converted to protonated form (HDPH) in the presence of water and show a hyperchromism in UV–Vis spectrum	[64]
Sudan-III and Alizarin Red S	Acetone Acetonitrile THF DMSO	Sudan-III: Up to 0.6820% v/v Up to 0.2911% Up to 0.3896% Up to 0.4773% Alizarin Red: Up to 0.6789% v/v Up to 0.7597% Up to 1.3954% Up to 7.2235%	Sudan-III: 0.0042% v/v 0.0119% 0.0058% 0.0299% Alizarin Red S: 0.0221% v/v 0.0498%, 0.0850%,, 0.5592%	NR	The deprotonated forms of Sudan-III and Alizarin Red S solutions are re-protonated by using a trace amount of water and show a dramatic changes in color	[65]
1,4-Dihydroxy-9,10-anthraquinone or quinizarin	Acetonitrile THF	0.097–1.157% v/v 0.096–1.046%	0.0011% v/v 0.0026%	NR	The deprotonated form of 1,4-dihydroxy-9,10-anthraquinone or quinizarin solution is re-protonated by using a trace amount of water and show a dramatic changes in color	[66]
Hydroxyl-containing polyimides	DMSO DMF	PI1-F: 0.025–0.5% v/v 0.0125–0.75 PI2-F: 0.025–0.5% v/v 0.0125–0.75%	PI1-F: 0.0035% v/v 0.0031% PI2-F: 0.00084%v/v 0.0015%	NR	The deprotonated forms of hydroxyl-containing polyimides solutions are re-protonated by using a trace amount of water and show a dramatic changes in color	[67]
Coumarin phenylsemicarbazones	Acetonitrile	Up to 0.36 v/v%	–	NR	The deprotonated form of coumarin phenylsemicarbazones is re-protonated by using a trace amount of water and shows a dramatic changes in color	[68]
Adenine-linked naphthalimide	Acetonitrile THF DMSO, Acetone	–	0.1086% v/v 0.1936% 0.4012% 0.3058%	NR	The deprotonated form of adenine-linked naphthalimide is re-protonated by using a trace amount of water and shows a dramatic changes in color	[69]
Diketopyrrolopyrrole-based luminogen	THF Acetone Acetonitrile	–	0.0064 v/v % 0.042 % 0.192%	NR	The deprotonated form of diketopyrrolopyrrole-based luminogen is re-protonated by using a trace amount of water and shows a dramatic changes in color	[70]
Indenopyrazine (1)/indenoquinoxaline (2) appended acylhydrazones	DMF	1: Up to 7.40% v/v 2: Up to 5.21%	1: 0.08732% v/v 2: 0.6759%	NR	The deprotonated form of 1 and 2 is re-protonated by using a trace amount of water and shows a dramatic changes in color	[71]

Table 2 (continued)

Applied material	Measured media	Linear range	LOD	RSD %	Remarks	Ref
Molecular probe bearing chalcone moiety	Acetone, Acetonitrile, Ethanol Isopropanol	Up to 10% v/v	0.20% v/v 0.38% 0.24% 0.09%	NR	Probe bearing chalcone moiety bind to metal nitrates selectively with remarkable color change from yellow to purple and the selected probe/$Ni(NO_3)_2$, can detect water content in organic solvents with re-changing color to yellow	[72]
Dabsyl-thiophene-based receptor DABT	THF Acetone Acetonitrile	0.0125–0.0780% w/w 0.0437–0.1980% 0.3055–2.4830%	0.0041%w/w 0.0144%	< 5.0%	The weak binding of Hg^{2+} with DABT in wet solvent is used a colorimetric probe for water detection	[73]
Azo@$AlPO_4$-5 nanochannel	Methanol Ethanol 1-Propanol 1-Butanol	Up to 12.9 wt% Up to 7.1% Up to 4.8% Up to 2.5%	–	NR	$AlPO_4$-5 facilitated the dissociation of water molecules chemisorbed in its framework. Azo dye is proton-sensitive. The generated H^+ protonated the encapsulated azo dye, resulting in a color change	[74]
Direct determination with NIR spectroscopy	Methyl ethyl ketone	Up to 0.25 wt%	~0.01 wt%	0.01%	–	[75]

NR not reported

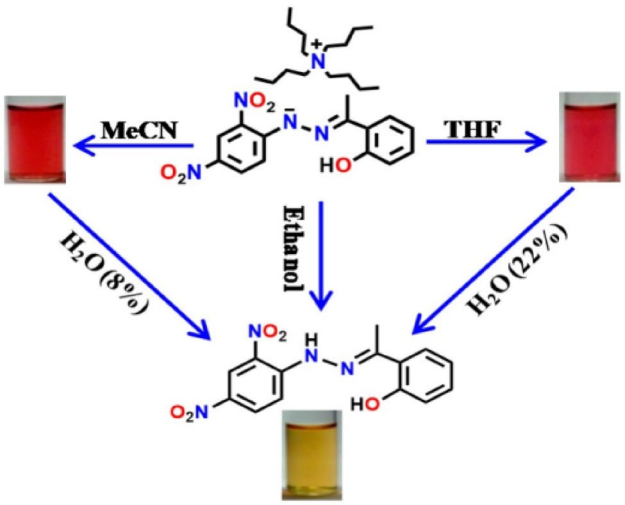

Fig. 7 The signaling of water content by DPH in acetonitrile and THF. Reproduced with permission from the publisher

chemisorbed in its framework. Azo dye is proton-sensitive. The produced H^+ protonated the encapsulated azo dye, leading to a color change which can be recognized with the naked eye. The degree of the color change of the azo dye would depend on the water amount in the nanochannel. Water content is investigated in methanol, ethanol, 1-butanol and 1-propanol. Sensitivity ranges for water determination are reported to be 0.0–12.9 wt% for methanol, 0.0–7.1 wt% for ethanol, 0.0–4.8 wt% for 1-propanol and 0.0–2.5 wt% for 1-butanol.

NIR spectrophotometric methods

van Kollenburg et al. [75] developed a handheld SCiO NIR spectroscopy for quantification of low-level of water contamination in methyl ethyl ketone with a precision of ~0.01 wt% in the 0–0.25 wt% range. They demonstrate that the regression vector of the partial least squares (PLS) model exhibits the water band as the main feature, proving the model's selectivity to the NIR water band. The benchtop FT-NIR system outperforms the SCiO sensor according to determination of trace amounts of water, which is to a large extent owing to the existing the strong water combination band ($\nu_{1,3} + \nu_2$) in the spectra of the benchtop FT-NIR system compared to the weaker second overtone of the O–H stretching band ($3\nu_{1,3}$) in the spectra of the SCiO probe. Comparing the systems with PLS regression only on the data from the 870–1070 nm spectral range (i.e., without considering the rest of the benchtop range), the data from the FT-NIR benchtop instrument resulted in models with slightly worse RMSEC (0.013 wt%) and RMSEP (0.101 wt%) values than those catch with the SCiO probe. It can be seen that the $3\nu_{1,3}$ peak

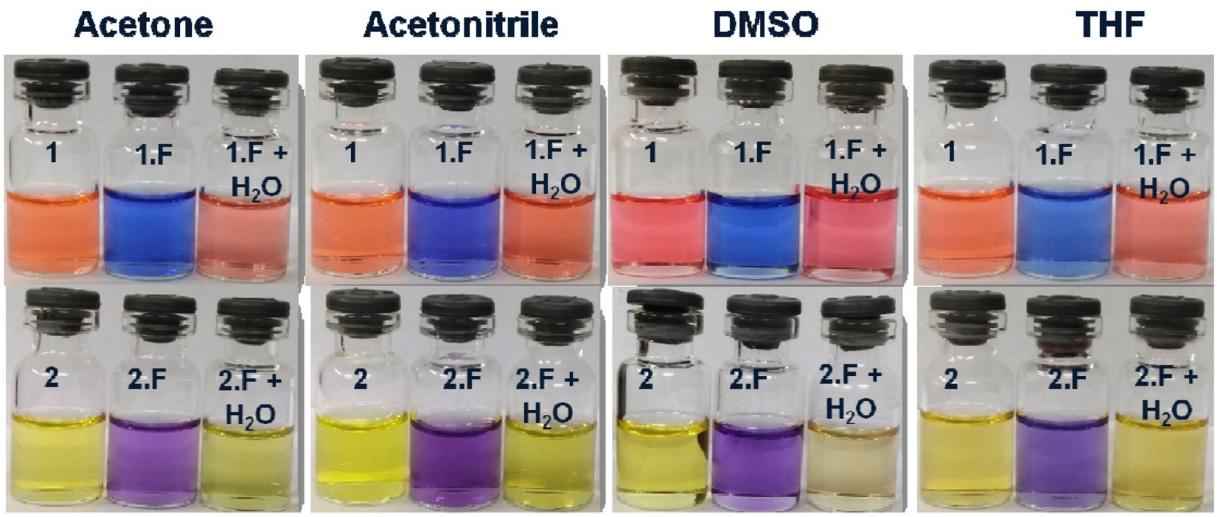

Fig. 8 Color changes of compounds 1 and 2 in acetone, acetonitrile, DMSO and THF after the addition of $[(nBu_4N)]F^-$ and their reversible color changes by the introduction of a trace amount of water in the solvents. Reproduced with permission from the publisher

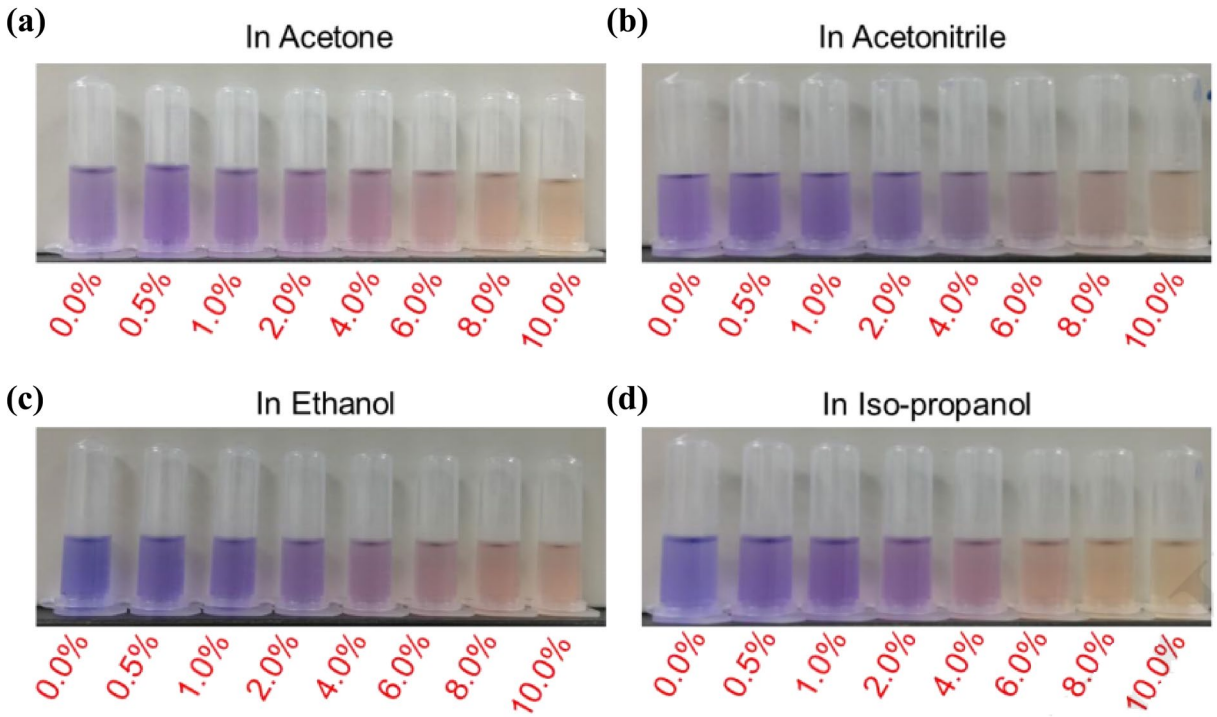

Fig. 9 The color changes of water titration toward two-component sensor C-1/$Ni(NO_3)_2$ in four organic solvents: **a** acetone, **b** acetonitrile, **c** ethanol and **d** isopropanol. The concentration of C-1 is 10 μM, and the concentration of $Ni(NO_3)_2$ is 50 μM, 20 μM, 20 μM and 20 μM in acetone, acetonitrile, ethanol and isopropanol, respectively. The number in red color shows the content of water in organic solvents (%). The photographs were taken after incubation for 10 min under room temperature. Reproduced with permission from the publisher

at 980 nm cannot be positively identified in the FT-NIR spectra, while the SCiO probe seems to be optimized in this region. An additional parameter is the modes of determinations were not the same for both instruments: SCiO determinations were collected by transflection (optical path length 2 cm) and the FT-NIR spectra by transmission (optical path length 6.8 mm).

Conclusion and future prospects

Development of inexpensive, rapid and sensitive alternative methods for the visualization as well as detection and determinations of water in organic solvents has been of great importance due to not only principal investigation in analytical photochemistry, chemistry and photophysics, but also their potential uses to monitoring systems of quality control and industry. Various research groups have reported different sensors for the quantification of water amount in organic solvents. The current article reviewed the published analytical techniques reported from 2016 until 2020. The literature is classified according to employed methodology, instrumentation and used materials for sensing, and the analytical features of all reported techniques are given for comparison and easy access. Based on the results of this review, various compounds such as dye, lanthanide, UC materials and nanomaterials with different mechanisms can be used for visualization of water contents utilizing spectroscopy instruments. Spectroscopy methods provide robust data and are reliable analytical methods; however, these methods generally show a low selectivity and sensitivity for analytical purposes. The recent efforts have focused on using nano- and UC materials to improve selectivity and sensitivity which can make future analytical techniques exploiting these materials a good alternative to used monitoring techniques, including Karl Fisher titration and electrochemical methods. Thus, the offering new materials-based optical probes are expected to be a popular topic for years to come. We hope this study persuades the community of scientific into designing real-time and sensitive water probes by using new materials and present a guidance in the choosing suitable sensing platform for future applications.

Acknowledgements This work was supported by Research Affairs of Tabriz University of Medical Sciences, under grant number 65523.

References

1. Y.Y. Liang, Anal. Chem. **62**(22), 2504–2506 (1990). https://doi.org/10.1021/ac00221a018
2. S.-I. Ohira, K. Goto, K. Toda, P.K. Dasgupta, Anal. Chem. **84**(20), 8891–8897 (2012). https://doi.org/10.1021/ac3024069
3. C.-G. Niu, P.-Z. Qin, G.-M. Zeng, X.-Q. Gui, A.-L. Guan, Anal. Bioanal. Chem. **387**(3), 1067–1074 (2007). https://doi.org/10.1007/s00216-006-1016-y
4. H.S. Jung, P. Verwilst, W.Y. Kim, J.S. Kim, Chem. Soc. Rev. **45**(5), 1242–1256 (2016). https://doi.org/10.1039/C5CS00494B
5. M.D. Ward, Chem. Soc. Rev. **26**(5), 365–375 (1997). https://doi.org/10.1039/CS9972600365
6. X. Liang, Q. Zhang, Sci. China Mater. **60**(11), 1093–1101 (2017). https://doi.org/10.1007/s40843-016-5170-2
7. A.C. Sedgwick, L. Wu, H.-H. Han, S.D. Bull, X.-P. He, T.D. James, J.L. Sessler, B.Z. Tang, H. Tian, J. Yoon, Chem. Soc. Rev. **47**(23), 8842–8880 (2018). https://doi.org/10.1039/C8CS00185E
8. S.V. Eliseeva, J.-C.G. Bünzli, Chem. Soc. Rev. **39**(1), 189–227 (2010). https://doi.org/10.1039/B905604C
9. Y. Hong, J.W. Lam, B.Z. Tang, Chem. Soc. Rev. **40**(11), 5361–5388 (2011). https://doi.org/10.1039/C1CS15113D
10. J. Hoche, H.-C. Schmitt, A. Humeniuk, I. Fischer, R. Mitrić, M.I. Röhr, Phys. Chem. Chem. Phys. **19**(36), 25002–25015 (2017). https://doi.org/10.1039/C7CP03990E
11. P. Kumar, S. Gadiyaram, D.A. Jose, Chem. Select **5**(34), 10648–10655 (2020). https://doi.org/10.1002/slct.202002530
12. Y. Ooyama, M. Hato, T. Enoki, S. Aoyama, K. Furue, N. Tsunoji, J. Ohshita, New J. Chem. **40**(9), 7278–7281 (2016). https://doi.org/10.1039/C6NJ01467D
13. T.I. Kimand, Y. Kim, Anal. Chem. **89**(6), 3768–3772 (2017). https://doi.org/10.1021/acs.analchem.7b00270
14. K. Kłucińska, P. Rzepiński, M. Mazur, M.K. Cyrański, K. Maksymiuk, A. Michalska, Food Anal. Methods **11**(2), 486–494 (2018). https://doi.org/10.1007/s12161-017-1019-7
15. X.-Y. Wang, C.-G. Niu, L.-Y. Hu, D.-W. Huang, S.-Q. Wu, L. Zhang, X.-J. Wen, G.-M. Zeng, Sens. Actuators B **243**, 1046–1056 (2017). https://doi.org/10.1016/j.snb.2016.12.084
16. K.-P. Wang, Y. Lei, J.-P. Chen, Z.-H. Ge, W. Liu, Q. Zhang, S. Chen, Z.-Q. Hu, Dyes Pigm. **151**, 233–237 (2018). https://doi.org/10.1016/j.dyepig.2018.01.004
17. Y. Zhang, C. Liang, S. Jiang, New J. Chem. **41**(16), 8644–8649 (2017). https://doi.org/10.1039/C7NJ01361B
18. W.E. Passos, I.P. Oliveira, F.S. Michels, M.A. Trindade, E.A. Falcão, B.S. Marangoni, S.L. Oliveira, A.R. Caires, Renew. Energy **165**, 42–51 (2021). https://doi.org/10.1016/j.renene.2020.11.041
19. D. Citterio, K. Minamihashi, Y. Kuniyoshi, H. Hisamoto, S.I. Sasaki, K. Suzuki, Anal. Chem. **73**(21), 5339–5345 (2001). https://doi.org/10.1021/ac010535q
20. D. Lu, Y. Tang, Y. Zheng, J. Fluoresc. **28**(6), 1269–1273 (2018). https://doi.org/10.1007/s10895-018-2300-x
21. B. Li, W. Wang, Z. Hong, E.-S.M. El-Sayed, D. Yuan, Chem. Comm. **55**(48), 6926–6929 (2019). https://doi.org/10.1039/C9CC02324K
22. J.-X. Wu, B. Yan, Dalton Trans. **46**(21), 7098–7105 (2017). https://doi.org/10.1039/C7DT01352C
23. Y. Dog, J. Cai, Q. Fang, X. You, Y. Chi, Anal. Chem. **88**(3), 1748–1752 (2016). https://doi.org/10.1021/acs.analchem.5b03974
24. J. Li, P. Du, J. Chen, S. Huo, Z. Han, Y. Deng, Y. Chen, X. Lu, Anal. Chem. **92**, 8974–8982 (2020). https://doi.org/10.1021/acs.analchem.0c00966
25. P. Majee, P. Daga, D.K. Singha, D. Saha, P. Mahata, S.K. Mondal, J. Photochem. Photobiol. A **402**, 112830 (2020). https://doi.org/10.1016/j.jphotochem.2020.112830
26. Z. Pan, Y. Wen, T. Wang, K. Wang, Y. Teng, K. Shao, J. Rare Earths **38**(4), 362–368 (2020). https://doi.org/10.1016/j.jre.2019.04.022
27. L. Zhang, X. Li, W. Wang, X. Zhao, X. Yan, C. Wang, H. Bao, Y. Lu, X. Kong, F. Liu, Nano Res. **13**(10), 2803–2811 (2020). https://doi.org/10.1007/s12274-020-2932-4
28. W. Wang, M. Zhao, L. Wang, H. Chen, Microchim. Acta **186**(9), 630 (2019). https://doi.org/10.1007/s00604-019-3744-7
29. J. Wei, H. Li, Y. Yuan, C. Sun, D. Hao, G. Zheng, R. Wang, RSC Adv. **8**(65), 37028–37034 (2018). https://doi.org/10.1039/C8RA06732E
30. J. Wei, Y. Yuan, H. Li, D. Hao, C. Sun, G. Zheng, R. Wang, New J. Chem. **42**(23), 18787–18793 (2018). https://doi.org/10.1039/C8NJ04365E

31. H.J. Lee, J. Jana, Y.-L.T. Ngo, L.L. Wang, J.S. Chung, S.H. Hur, Mater. Res. Bull. **119**, 110564 (2019). https://doi.org/10.1016/j.materresbull.2019.110564
32. C. Ye, Y. Qin, P. Huang, A. Chen, F.-Y. Wu, Anal. Chim. Acta **1034**, 144–152 (2018). https://doi.org/10.1016/j.aca.2018.06.003
33. Z. Li, X. Chen, L. Yu, H. Li, L. Chen, Q. Kang, D. Shen, Microchim. Acta **187**(10), 1–12 (2020). https://doi.org/10.1007/s00604-020-04551-w
34. J. Wang, J. Wang, W. Xiao, Z. Geng, D. Tan, L. Wei, J. Li, L. Xue, X. Wang, J. Zhu, Anal. Methods (2020). https://doi.org/10.1039/D0AY00485E
35. Y. Huang, W. Liu, H. Feng, Y. Ye, C. Tang, H. Ao, M. Zhao, G. Chen, J. Chen, Z. Qian, Anal. Methods **88**(14), 7429–7434 (2016). https://doi.org/10.1021/acs.analchem.6b02149
36. D. Chao, W. Lyu, Y. Liu, L. Zhou, Q. Zhang, R. Deng, H. Zhang, J. Mater. Chem. C **6**(28), 7527–7532 (2018). https://doi.org/10.1039/C8TC02184H
37. M. Zhao, H. Feng, X. Zhang, H. Ao, Z. Qian, Analyst **142**(24), 4613–4617 (2017). https://doi.org/10.1039/C7AN01542A
38. A. Senthamizhan, D. Fragouli, B. Balusamy, B. Patil, M. Palei, S. Sabella, T. Uyar, Nanoscale Adv. **1**(11), 4258–4267 (2019). https://doi.org/10.1039/C9NA00493A
39. F. Gao, F. Luo, X. Chen, W. Yao, J. Yin, Z. Yao, L. Wang, Microchim. Acta **166**(1–2), 163–167 (2009). https://doi.org/10.1007/s00604-009-0180-0
40. H.-Q. Yin, J.-C. Yang, X.-B. Yin, Anal. Chem. **89**(24), 13434–13440 (2017). https://doi.org/10.1021/acs.analchem.7b03723
41. P. Kumar, R. Kaushik, A. Ghosh, D.A. Jose, Anal. Chem. **88**(23), 11314–11318 (2016)
42. J. Hu, X. Yu, X. Zhang, C. Jing, T. Liu, X. Hu, S. Lu, K. Uvdal, H.-W. Gao, Z. Hu, Spectrochim. Acta A **241**, 118657 (2020). https://doi.org/10.1021/acs.analchem.6b03949
43. N.I. Georgiev, P.V. Krasteva, V.B. Bojinov, J. Lumin. **212**, 271–278 (2019). https://doi.org/10.1016/j.jlumin.2019.04.053
44. H. Sun, X.-X. Tang, B.-X. Miao, Y. Yang, Z. Ni, Sensors Actuators B. **267**, 448–456 (2018). https://doi.org/10.1016/j.snb.2018.04.022
45. P. Shen, M. Li, C. Liu, W. Yang, S. Liu, C. Yang, J. Fluoresc. **26**(1), 363–369 (2016). https://doi.org/10.1007/s10895-015-1722-y
46. M. Cigáň, M. Horváth, J. Filo, K. Jakusová, J. Donovalová, V. Garaj, A. Gáplovský, Molecules **22**(8), 1340 (2017). https://doi.org/10.3390/molecules22081340
47. L. Chen, J.-W. Ye, H.-P. Wang, M. Pan, S.-Y. Yin, Z.-W. Wei, L.-Y. Zhang, K. Wu, Y.-N. Fan, C.-Y. Su, Nature Commun. **8**(1), 1–10 (2017)
48. H.T. Bui, J.M. Lim, D.K. Mai, H. Kim, H.-J. Kim, H.J. Kim, S. Cho, Dyes Pig. **176**, 108194 (2020). https://doi.org/10.1016/j.dyepig.2020.108194
49. K. Zhang, T.-T. Chen, Y.-J. Shen, L.-F. Zhang, S. Ma, Y. Huang, Sensors Actuators B **311**, 127887 (2020). https://doi.org/10.1016/j.snb.2020.127887
50. T. Chen, Z.-Q. Chen, W.-L. Gong, C. Li, M.-Q. Zhu, Mater. Chem. Front. **1**(9), 1841–1846 (2017). https://doi.org/10.1039/C7QM00172J
51. T. Enoki, Y. Ooyama, Dalton Trans. **48**(6), 2086–2092 (2019). https://doi.org/10.1039/C8DT04527E
52. W.Y. Kim, H. Shi, H.S. Jung, D. Cho, P. Verwilst, J.Y. Lee, J.S. Kim, Chem. Commun. **52**(56), 8675–8678 (2016). https://doi.org/10.1039/C6CC04285F
53. Y. Chen, C. Zhang, J. Xie, H. Li, W. Dai, Q. Deng, S. Wang, Anal. Chim. Acta **1109**, 114–121 (2020). https://doi.org/10.1016/j.aca.2020.03.003
54. Z. Wang, G. Wang, X. Chang, K. Liu, Y. Qi, C. Shang, R. Huang, T. Liu, Y. Fang, Adv. Funct. Mater **29**(44), 1905295 (2019). https://doi.org/10.1002/adfm.201905295
55. X. Zhao, S. Yang, J. Lumin. **220**, 116993 (2020). https://doi.org/10.1016/j.jlumin.2019.116993
56. J. Nootem, C. Sattayanon, S. Namuangruk, P. Rashatasakhon, W. Wattanathana, G. Tumcharern, K. Chansaenpak, Dyes Pigm. **181**, 108554 (2020). https://doi.org/10.1016/j.dyepig.2020.108554
57. M. Tanioka, S. Kamino, A. Muranaka, Y. Shirasaki, Y. Ooyama, M. Ueda, M. Uchiyama, S. Enomoto, D. Sawada, Phys. Chem. Chem. Phys. **19**(2), 1209–1216 (2017). https://doi.org/10.1039/C6CP06808A
58. X. Du, R. Fan, L. Qiang, Y. Song, K. Xing, W. Chen, P. Wang, Y. Yang, Inorg. Chem. **56**(6), 3429–3439 (2017). https://doi.org/10.1021/acs.inorgchem.6b02963
59. C. Yang, X. Wang, Z. Xu, M. Wang, Sensors Actuators B **245**, 845–852 (2017). https://doi.org/10.1016/j.snb.2017.01.147
60. S. Kumar, S. Maji, K. Sundararajan, K. Sankaran, Luminescence **33**(3), 611–615 (2018). https://doi.org/10.1002/bio.3453
61. P. Yuvaraj, J. Ajantha, S. Easwaramoorthi, J.R. Rao, New J. Chem. **44**(16), 6566–6574 (2020). https://doi.org/10.1039/D0NJ00636J
62. K. Zargoosh, M. Barmaki, A. Abdolmaleki, K.F. Tadavani, J. Iran. Chem. Soc. **17**(4), 923–933 (2020). https://doi.org/10.1007/s13738-019-01823-y
63. K. Zargoosh, R. Reisi Oshtorjani, K. Karami, S. Hashemi, Luminescence **35**(1), 69–78 (2020). https://doi.org/10.1002/bio.3697
64. K. Tiwari, M. Mishra, S. Singh, V.P. Singh, ChemistrySelect **5**(30), 9547–9553 (2020). https://doi.org/10.1002/slct.202002005
65. P. Kumar, R. Sakla, A. Ghosh, D.A. Jose, Appl. Mater. Interfaces **9**(30), 25600–25605 (2017). https://doi.org/10.1021/acsami.7b05335
66. P. Kumar, A. Ghosh, D.A. Jose, Analyst **144**(2), 594–601 (2019). https://doi.org/10.1039/C8AN01042K
67. Y. Wu, J. Ji, Y. Zhou, Z. Chen, S. Liu, J. Zhao, Anal. Chim. Acta (2020). https://doi.org/10.1016/j.aca.2020.02.043
68. M. Cigáň, J. Gašpar, K. Gáplovská, J. Holekšiová, K. Jakusová, J. Donovalová, V. Garaj, H. Stankovičová, New J. Chem. **40**(10), 8946–8953 (2016). https://doi.org/10.1039/C6NJ01639A
69. C. Pati, R. Raza, K. Ghosh, Spectrochim. Acta A **229**, 117910 (2020). https://doi.org/10.1016/j.saa.2019.117910
70. F. Wu, L. Wang, H. Tang, D. Cao, Anal. Chem. **91**(8), 5261–5269 (2019). https://doi.org/10.1021/acs.analchem.9b00032
71. K. Santhiya, S.K. Sen, R. Natarajan, B. Dyes Pigm. **185**, 108891 (2021). https://doi.org/10.1016/j.dyepig.2020.108891
72. J. Tan, X. Wang, Q. Zhang, H. Zhou, J. Yang, J. Wu, Y. Tian, X. Zhang, Sensors Actuators B **260**, 727–735 (2018). https://doi.org/10.1016/j.snb.2017.12.186
73. P. Kumar, D.A. Jose, Anal. Chim. Acta **1136**, 178–186 (2020). https://doi.org/10.1016/j.aca.2020.09.058
74. H. Yoo, H.S. Kim, J. Mater. Chem. C **7**(24), 7336–7343 (2019). https://doi.org/10.1039/C9TC01767D
75. G.H. van Kollenburg, H.-J. van Manen, N. Admiraal, J. Gerretzen, J.J. Jansen, Talanta **12**, 2020 (1865). https://doi.org/10.1016/j.talanta.2020.121865